



**HAL**  
open science

## **Antcar: Simple Route Following Task with Ants-Inspired Vision and Neural Model**

Gabriel Gattaux, Roxane Vimbert, Antoine Wystrach, Julien R. Serres,  
Franck Ruffier

► **To cite this version:**

Gabriel Gattaux, Roxane Vimbert, Antoine Wystrach, Julien R. Serres, Franck Ruffier. Antcar: Simple Route Following Task with Ants-Inspired Vision and Neural Model. 2023. hal-04060451

**HAL Id: hal-04060451**

**<https://hal.science/hal-04060451>**

Preprint submitted on 17 Apr 2023

**HAL** is a multi-disciplinary open access archive for the deposit and dissemination of scientific research documents, whether they are published or not. The documents may come from teaching and research institutions in France or abroad, or from public or private research centers.

L'archive ouverte pluridisciplinaire **HAL**, est destinée au dépôt et à la diffusion de documents scientifiques de niveau recherche, publiés ou non, émanant des établissements d'enseignement et de recherche français ou étrangers, des laboratoires publics ou privés.



Distributed under a Creative Commons Attribution - NonCommercial 4.0 International License

# Antcar: Simple Route Following Task with Ants-Inspired Vision and Neural Model

G. Gattaux<sup>1,\*</sup>, R. Vimbert<sup>1</sup>, A. Wystrach<sup>2</sup>, J.R. Serres<sup>1,3</sup> and F. Ruffier<sup>1</sup>

**Abstract**—The goal of this project is to develop a new method of Route following for mobile robots in a GNSS-denied environment like urban canyons or indoor. We used a robust biologically constrained neural model inspired by ants developed previously in simulation to assess the familiarity index of a panorama. A visual compass algorithm consists in determining the orientation of the maximum familiarity index with respect to the learned panoramas along a path. A car-like robot was equipped with a 220° fisheye camera. The visual compass algorithm used low resolution images of 44x44 pixels (5°/pixel) indoors and outdoors to determine the direction to follow the previously visually-learned path. Finally, the car-like robot was automated to recall the learned path indoors. The biologically constrained neural model compressed the visual information with a high efficiency so that the visual memory has a very low footprint of a few tens of kilobits that does not depend directly on the path length.

## I. INTRODUCTION

Three questions can represent the navigation process: "Where am I?", "Where am I going?" and "How do I get there?" [1]. Standalone autonomous navigation is one of the greatest challenges in robotics [2]. As an example, mapping in robotics requires a significant effort and a large memory, like the use of Simultaneous Localization And Mapping (SLAM) equipped with a Light Detection And Ranging (LiDAR) [3] or stereoscopic vision [4]. In the same way, the localization requires bigger means as the Global Positioning System (GPS) and the Real-Time Kinematic positioning (RTK) to obtain accuracy up to centimeters [5] or reasonable means as the estimations and derivation via the Inertial Measurement Unit (IMU) [6] or the odometer, but drifting in time.

The insects-based algorithms, from the brains to the mechanical movements, are full of knowledge and further robotics realizations will experience a tour de force in the scientific area of autonomous navigation [7], [8] and [9]. Ants, like *Cataglyphys velox* or *Melophorus bagotis*, which are recognized for their visual-based navigation skills are capable, with a single learning trial, to memorize long routes between points of interest like a feeder and their nest (see Fig.4a in [10]). They utilize several instruments of navigation to explore, then to return to the nest as we can see it through its unified navigation model [11] or multimodal model [12]. It appears that ants have a constant recalling process from the road learned dues to visual cues or Path Integrator (PI) [13]. As concluded in [10] the route recalling process is working

even if the global PI is "disabled" in ants brain, visual cues are therefore important for this process.

Ants can see the world through two primary channels, green and ultraviolet (UV) [14], [15]. The key characteristic of these insects' visual system is their low resolution (5°/pixel to 10°/pixel) with a wide field of view (almost 330°). A previous study [16] indicated that thanks to their reduced resolution, they are untangled with branches, leaves or other ephemeral cues.

The connectomics data is the comprehensive maps of connections within an organism's nervous system [17]. To pre-process the visual information, ants use a lateral inhibition, considered as an edge detection [18]. They transform those views in Neural Projection (PN), PN are interneurons that transmit the sensors' information to the calyxes of the Mushroom Bodies (MBs). In others words, PNs (or sensory information) are learned in the memory center, called MBs [19]. The MBs were accurately described in insects starting in 2003 with Heisenberg [20] using the fly *Drosophila melanogaster* and his "Olfactory Memory Circuit Model." The information is therefore encoded sparingly, without snapshot storage, in the case of visual sensory message [21]. Inside an MB, the intrinsic neurons in charge of learning are called the Kenyon Cells (KCs). Bigger KC' number do not necessary means that the insect is best suited for recognition. For example, associative learning (defined as learning about the relationship between two separate stimuli, the stimuli can be abstract like time, location or context) can be achieved in MB containing only a few hundred KC, even if the bees have 170,000 KCs [22].



Fig. 1. Antcar mobile robot fitted with fisheye camera at 220° elevation field of view sky oriented in grassy environment. © Cyril Frésillon / ISM / CNRS Photothèque.

<sup>1</sup> Aix Marseille Univ., CNRS, ISM, Marseille, France

<sup>2</sup> CRCA, CBI, CNRS, Toulouse III Univ., Toulouse, France

<sup>3</sup> Institut Universitaire de France (IUF), Paris, France

\* Corresponding author: gabriel.gattaux@univ-amu.fr

One hypothesis implemented in simulation is that their route-following behavior is based on a Visual Compass (VC). VC consists in determining the direction (by scanning) that maximize the familiarity index with respect to the views learned along the path [23]. This VC model can be implemented by an Image Difference Function (IDF) known as Perfect Memory (PM) which consist of differentiate pixelwise the current image from the learned images stocked. IDF allows us to have a familiarity-like index compared to the learned path. However, certain neural models allow us to encode the visual memory and therefore not to store images, while still having this familiarity index. This is, for example, the case with Infomax [24], Multi layer perceptron (MLP) or our famous MB model. Few VC models exist in simulation:

- This study investigates the difference (in time and performance) between PM and Infomax [25].
- Using MB model, PM and Infomax, they are able to recover the route learned [26].
- They compare here simple MLP vs PM [27].
- For UAV this time, they compare Infomax vs PM [28].

Very few VC models exist in real environments :

- Indoor environments with PM, they are able to recognize and reach their learned route [29].
- Outdoor with closed loop control, they compare PM vs Infomax [30].
- Indoor with MB model, they investigate the limits of their MB model [31].
- A dataset was settled up by [32] and they also compared the following papers [26];[31];[25].

Klinokinesis (direct gradient descent without the process of VC) could be a useful algorithm to reach the best familiarity in a picture [33] without the calculation time of VC.

The visual system and the neural network on board the mobile robot AntCar (Fig. 1) try to mimic faithfully desert ants' navigation techniques based on visual cues. To avoid or to combine the use of GPS, LiDAR and any other energy consuming sensors, which are sensitive to spoofing, jamming, or dazzling on board an autonomous mobile robot for route following in complex environments. To situate our work, we present knowledge about the capabilities of the VC coupled with the MB model to work in any type of environment, indoors (visually controlled environments) and outdoors (semi-wild environments). There is a perspective for this coupled model (VC and MB) to be readily implemented in robots navigating in the real world, indoor (shown) and outdoor (not shown), what has never been done before. The goals are to obtain a closed-loop behavior that resembles the behaviors observed in ants (see Fig.4a in [10]) based solely on visual cues.

This study is structured as follows: section II provides a brief description of the mobile robot and its visual system. The visual memorization using an MB model is introduced in section III. Then, indoor out outdoor VC results are described in section IV, and a simple real time controller based on VC and MB are described in section V. Finally, a conclusion and future works are developed in section VI.

## II. ANT-CAR SYSTEM AND VISION

### A. Experimental Setup



Fig. 2. Panoramic picture of the indoor visual scene in the AVM, man point of view.

To implement this visual learning strategy, we used the PiRacer robot purchased on [www.waveshare.com](http://www.waveshare.com). The car-like mobile robot is 40cm-long and made of four wheels. Each of the rear wheels is driven by a DC motor. A servo motor is connected to the two front wheels to steer the robot. The chassis of the robot is made of aluminum to ensure resistance to small shocks. The processing and computation are done by a *Raspberry Pi 4B* that communicates by I2C with an external hat configured with PCA9685 module. In the Mediterranean flight arena (AVM) Fig. 2, the ground truth is extracted from a VICON motion capture system completed with 17 infrared cameras capturing 8 x 6 x 6 m. To have ground truth in different place, the Antcar is equipped with RP LIDAR A1 as well as an MPU6050, hector SLAM ROS packages have been used for pose estimation. The whole data are transmitting through ROS network as seen in the Fig. 3.

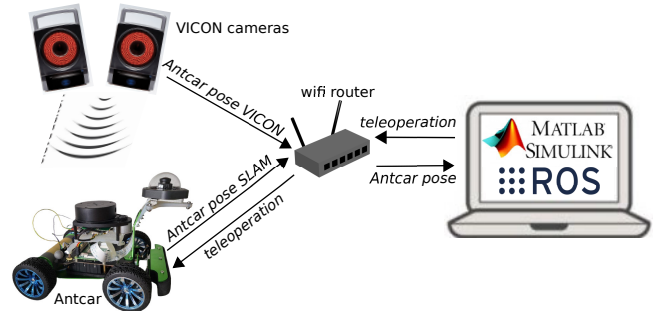


Fig. 3. The ground truth is possible thanks to the motion capture system, the five reflective markers and the hector SLAM ROS packages.

### B. Image processing steps

The acquisition part is made by an *Entaniya* fisheye camera with a 220° angle of view for elevation and 360° azimuth. This camera is fixed on the head of the robot, Fig. 1. It has a frame rate of 30Hz and a glass cap covers the camera for optimal rain/dust resistance. The image was used as it is without performing any panoramic expansion for the purpose of saving computation time. The steps to manage an ant-like view are explained below by comparing the real mechanisms to the imitating one.

#### 1) Acquisition :

- Natural : Compound eye capturing environment at low resolution 5°/pixels.

- Robotic : *Entaniya* fisheye camera with green channel at 160 x 160 pixels, then subsampled to 44 x 44 pixels.
- 2) Edge extraction :
- Natural : Lateral inhibition.
  - Robotic : Sobel filter is applied on the 44 x 44 pixels image.
- 3) Image encoding :
- Natural : The visual information is encoded through the PN.
  - Robotic : With aim to recreate the PN, scroll the image in a vector from top left to bottom right with the condition where the pixel exist if it is inside a circle of 22 pixels radius starting from the center of the image. Corresponding to the PN creation.

An example of such processing results are showed in the Fig. 4 for the indoor and outdoor environment. Those images will further represent the corresponding indoor and outdoor environment for the results part.

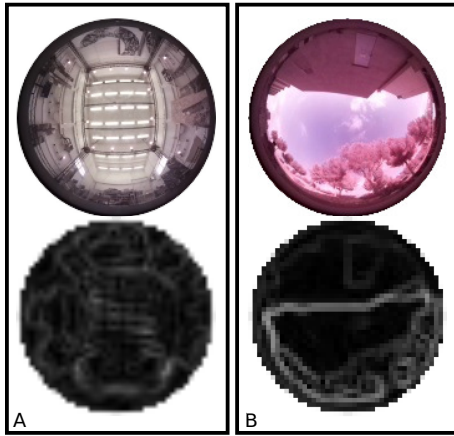


Fig. 4. Pictures from Antcar point of view with fisheye deformation and transformations. A) Indoor photo of the AVM. B) Outdoor photo of the Gateway to the National Park of the Calanques of Marseilles. (Up) Image taken at 160 x 160 px. (Down) Subsampled at 44 x 44 then Sobel filtered.

### III. VISUAL MEMORIZATION USING MUSHROOM BODIES MODEL

The Fig. 5 represents a simplified MB model which illustrate the different stages of the image learning process. The model used here has been derived from [26]. After the image treatment process, the PNs are projected to ten of thousands Kenyon cells in the mushroom bodies through fixed but pseudo-random connections.

#### A. Initialisation

The input of the neural model is a *PN*. Let us define  $N = 1078$ , the size of the PN vector, which is the number of pixels inside the useful and processed image. The number of KC arbitrary choose as  $n = 10\ 000$ . Read below  $i$  as being the  $i^{th}$  value of a vector. Firstly, the learning process is defined by successive steps, illustrated by the Fig. 6 as well as the recognition process in Fig. 7. The connectivity matrix

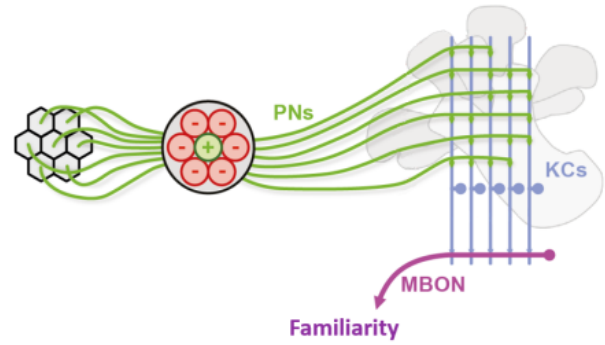


Fig. 5. Mushroom bodies model from the compound eye to Mushroom bodies output neurons (MBON), including the Kenyons Cells (KCs). Adapted from [34]

*PN-to-KC* is kept in memory, it is a constant matrix that has to be stored continuously without changing values, it only depends on the model parameter.

#### B. Learning (or memorization) process

At the end of the learning, the vector *SW* have to be stored and changed dynamically, Fig. 6. It is the *SW* information (vector of  $n \times 1$ ) that will be compared to know if we recognize the route. The path memory is encoded in this vector. As a result, the memory's size is not a direct function of the number of images learned, but depends on the number of KC.

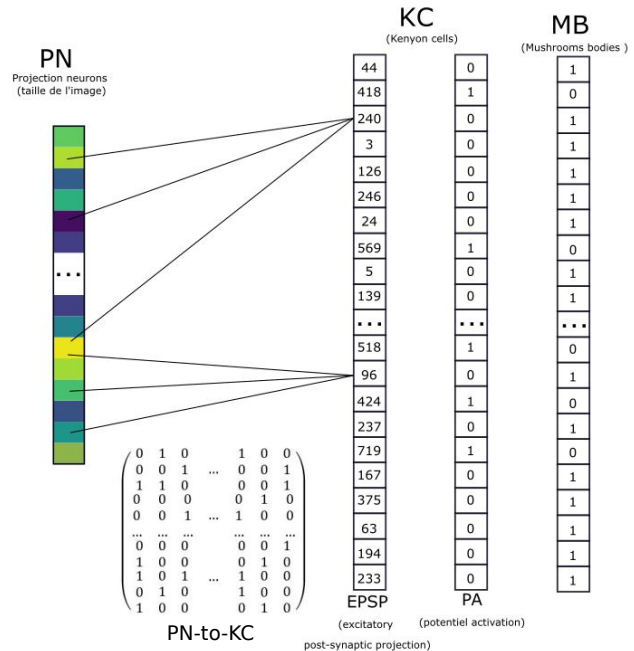


Fig. 6. The learning (or memorization) process takes as input an image or a series of coarse images organized in an elongated column vector called PN. Due to the fixed pseudo-random PN-to-KC connectivity, each image triggers a unique pattern of activity in the Kenyon cells' population. Kenyon's cells that receive strong excitatory post-synaptic potential (EPSP) are considered to fire one action potential (PA). The output connection of the KC that fired during learning is switched-off (SW=0). As novel images are learned, more and more KC's output are thus switched to zero.

- 1) Initialization
  - a) Creation of the connectivity matrix **PN-to-KC**: Binary matrix of size  $N*n$ . Each row is filled by a defined percentage of 1, here 5 by an arbitrary choice.
  - b) Creation of the synaptic weight vector **SW** : a Binary vector of size  $n$  initialized to 1 everywhere.
- 2) Creation of the neural projection **PN** : This step corresponds to the part explained previously, the transformation of the image into a vector of size  $N$ .
- 3) KC processing : Multiplication of the vector **PN** by the connectivity matrix **PN-to-KC** which results in a vector called **EPSP** (Excitatory Post-Synaptic Projection).
- 4) Binary vector Activation potential **PA** of size  $n$  : Passes to 1 for the 5% of the largest values of the vector **EPSP**, the others to 0.
- 5) If **PA(i) = 1**, switch the value **SW(i)** to 0. So if **PA(i) = 0**, **SW(i) = 1**.
- 6) Repeat steps 2 through 5 for each image to be learned.

### C. Recognition (or exploitation) process

Now, each PN-transformed image can be compared to the stored memory (**SW**) corresponding to a previously learned path. The result of this recognition process is a familiarity index. As seen on the Fig. 7, the more the index tends towards 0 the more the image is familiar and conversely (unfamiliarity is 1-familiarity).

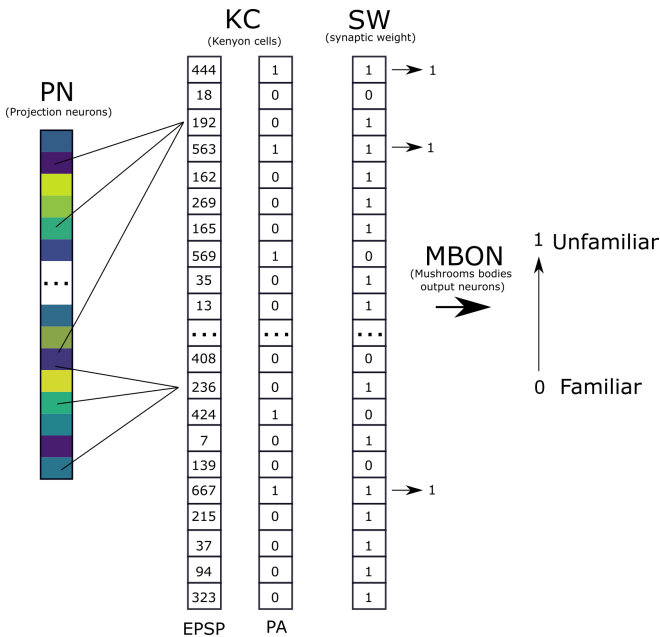


Fig. 7. The recognition process takes as input the current image organized in an elongated column vector called PN which is multiplied by the PN-to-KC connectivity matrix as during training, resulting in a pattern of activation in the Kenyon Cells specific to the current image. The firing KCs (PA=1) activate the output neuron (MBON) only if their output connection has not been switched off during the learning stage (SW=1). MBON activity can thus be implemented as a logical PA=1 AND SW=1 operation, which results in an estimate of current image's unfamiliarity.

- 1) Initialization
  - a) Recovery of the connectivity matrix **PN-to-KC** from the learning phase
  - b) Retrieve the vector **SW** of the learning phase
- 2) Creation of the neural projection: Transformation of the image into a vector of size  $N$ .
- 3) KC processing: Same as step 3 of the learning phase.
- 4) Binary vector Potential of activation **PA** of size  $n$  : Same as step 4 of the learning phase.
- 5) Here, we compare the current values of **PA(i)** and the learned values of **SW(i)**. That is, if **PA(4) = 1** and **SW(4) = 1** then, we increment a temporary variable **tmp = tmp + 1** (logical AND). Otherwise, if **PA(4) = 0** and **SW(4) = 1** then nothing is incremented.
- 6) Once this operation is carried out, normalize the result by  $n$  as **MBON = tmp / n**. Where **MBON** is the non-familiarity index ranging from 0 to 1 for the image currently compared to a memory learned in the MB (**SW**).
- 7) Repeat steps 2 through 6 for each image to be compared.

### IV. RESULTS 1 : INDOOR AND OUTDOOR VISUAL COMPASS WITH MB MODEL

Firstly, the VC algorithm was tested in diverse environments along with the MB model described in Section III. The Fig. 8 show the familiarity computation over 360° for a learned direction of vision in the AVM environment. This clearly shows the most familiar image is the one in the direction of vision learned (red arrow).

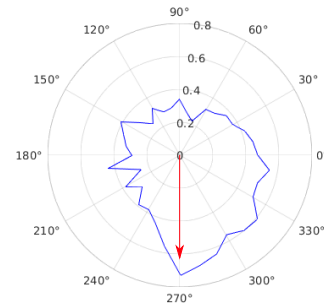


Fig. 8. Familiarity computed by the recognition process in III-C with the MB model over 360 degree (blue line). The learned image was in the direction of 270 degree in the AVM (red arrow). The internal radius length is the familiarity index value.

For the result in Fig. 9 and Fig. 10, the images are learned every 10 cm in a memory called (5 Hz at a speed of 0.5 m/s). In order to have smoothed results, a Savitsky-Golay filter of order 1 and window 7 is applied on the unfamiliarity indices. An interpolation of the results was also undertaken.

For a robotic purpose, there can be two useful outputs. On one hand, the direction that maximize the familiarity index by rotating *in silico* in steps of 1 degree over 360 degrees, i.e. the VC. We have shown experimentally in Fig. 9 that the most familiar direction was to choose the direction parallel to the learned path, whether outside or inside, which consist

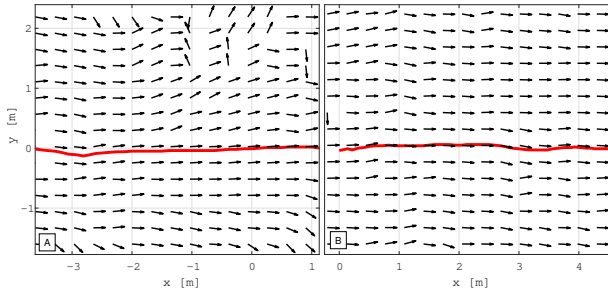


Fig. 9. The most familiar direction: (A) Indoor. (B) Outdoor. The red lines represent the learned visual routes. The black arrow represents the direction maximizing familiarity by scanning *in silico* at different position and whatever orientation.

in orientation error. The information here allows us to know in which relative direction the agent must go to follow its path parallel to the learned path. On the other hands, the familiarity index in the best direction is measured to allow an estimation of the position error between the learned path and our current position in Fig. 10

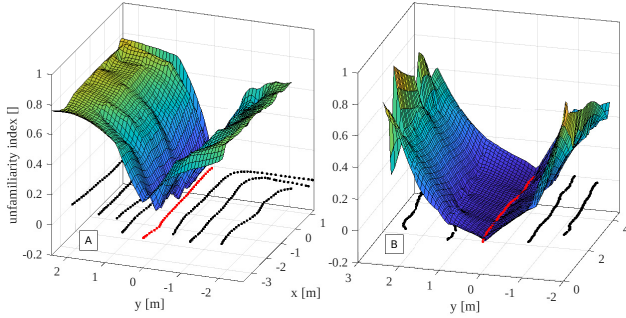


Fig. 10. Unfamiliarity over 2D space: The colors gradient represents the unfamiliarity index against the best direction of vision from the Mushroom Bodies Output Neuron (MBON). (A) Indoor. (B) Outdoor.

The improvement of the skyline contrast appears to decrease the gradient values of these "canyon" shapes. These results in a recognition that extends around the path compared to inside. The AntCar performance is slightly improved by enhancing the contrast of the skyline: results in Fig. 9.B and 10.B are indeed better than in Fig. 9.A and 10.A due to the open space that strongly improved the familiarity index's map.

## V. RESULTS 2 : INDOOR SIMPLE CONTROLLER BASED ON VISUAL COMPASS

This result shows a simple proportional controller based on VC output along with MB model for learning and recognition process in the AVM. The image resolution was about 44 x 44 pixels, the number of KC equals 10 000, to be able to learn the path without necessarily demanding too much time. To have faster computation time, the scanned beam was not 360° in steps of 1° but  $\pm 100^\circ$  in steps of 10°. The proportional gain  $K_p = 1.3$ . The error considered here is only the error of heading between the current view and the visual direction of the path learned, noted  $\theta_{max}$ . The output of the algorithm is

then a relative desired heading, considered here as the error we tend to minimize. The error has a refreshing rate of 3 Hz. The proportional heading controller is described in Eq. 1

$$\theta = K_p * \theta_{max} \quad (1)$$

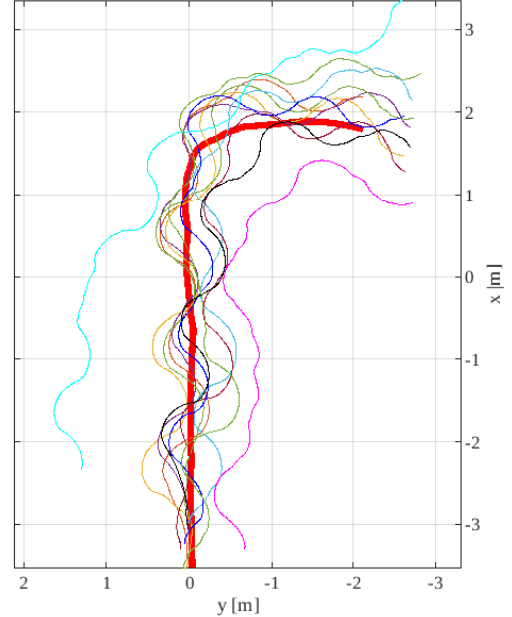


Fig. 11. Real time trials with visual compass based controller. The learning route is in red

Following the implementation of this algorithm in real time, we can see on the Fig. 11 the learning route in red and then the successive eleven routes that the robot follows autonomously thanks to the visual compass algorithm coupled to the internal memory encoded in an MB model. The learning road (red) and replacement in the initial condition (not plotted) were done by human teleoperation. This last experiment shows us that the algorithm is relatively slow (3Hz) because it must scan its environment (i.e. internally rotate the image and compare it to the encoded memory). The oscillations are mainly due to the Ackerman system coupled with a slow refreshing rate, which gives the errors at a previous location and not the current one. We can also see the agent does not join the route well when there is a deviation in its initial position compared to the learned route. The robot is not capable to rejoin the route learned if it is positioned far from it. However, we can see some robustness of the route following, as the agent moves in a corridor of 1 m width centered on the learned route Fig. 11.

## VI. CONCLUSION AND FUTURE WORKS

As seen in the previous results, the recognition process is rotation-variant, in other words, a big familiar index appear when the direction of vision is the same as the direction of vision learned. This specificity is used by the VC. This study

show the potential for further improvements or uses with the VC output along with the MB model and demonstrated the feasibility of such an algorithm on a simple car-like robot, only equipped with a Raspberry Pi 4 control board. This model could be the first step of a useful additional backup for robotic route following task in complex environments.

One limitation is the algorithm leads to a parallel route and therefore does not allow for accurate route recovering if the initial condition is not on the learned route. An idea could be to implement a descent gradient algorithm after the VC process to achieve the route following not only parallel to the learned path, but for returning to it, to solve the registration problem.

From a biological point of view, a question remains unanswered, how do the ants reach this road when they are relatively far from it. Several hypotheses have been proposed, notably the possibility that ants use a different navigation strategy on and off the road [35] but also lately the opposition process in visual memory [34].

#### ACKNOWLEDGMENT

We thanks C.Coquet and A. Ndoye for the use of the motion capture system of the AVM. This research was supported by the Agence de l’Innovation de Défense (AID), CNRS, Aix Marseille University, the Provence-Alpes-Côte d’Azur region. This work has been partially supported by ROBOTEX 2.0 (Grants ROBOTEX ANR-10-EQPX-44-01 and TIRREX ANR-21-ESRE-0015).

#### REFERENCES

- [1] B. Rahmani, A. Putra, A. Harjoko, and T. Priyambodo, “Review of vision-based robot navigation method,” *IAES International Journal of Robotics and Automation (IJRA)*, vol. 4, p. 254, 12 2015.
- [2] G.-Z. Yang, J. Bellingham, P. E. Dupont, P. Fischer, L. Floridi, R. Full, N. Jacobstein, V. Kumar, M. McNutt, R. Merrifield *et al.*, “The grand challenges of science robotics,” *Science robotics*, vol. 3, no. 14, p. eaar7650, 2018.
- [3] P. Newman, D. Cole, and K. Ho, “Outdoor slam using visual appearance and laser ranging,” in *Proceedings 2006 IEEE International Conference on Robotics and Automation, 2006. ICRA 2006.* IEEE, 2006, pp. 1180–1187.
- [4] B. Kitt, A. Geiger, and H. Lategahn, “Visual odometry based on stereo image sequences with ransac-based outlier rejection scheme,” in *2010 IEEE intelligent vehicles symposium.* IEEE, 2010, pp. 486–492.
- [5] Y. Feng, J. Wang *et al.*, “Gps rtk performance characteristics and analysis,” *Positioning*, vol. 1, no. 13, 2008.
- [6] K. Saadeddin, M. F. Abdel-Hafez, and M. A. Jarrah, “Estimating vehicle state by gps/imu fusion with vehicle dynamics,” *Journal of Intelligent & Robotic Systems*, vol. 74, no. 1, pp. 147–172, 2014.
- [7] G. de Croon, J. Dupeyroux, S. Fuller, and J. Marshall, “Insect-inspired ai for autonomous robots,” *Science Robotics*, vol. 7, no. 67, p. eabl6334, 2022.
- [8] B. Webb, “Robots with insect brains,” *Science*, vol. 368, no. 6488, pp. 244–245, 2020.
- [9] G.-Z. Yang, J. Bellingham, P. E. Dupont, P. Fischer, L. Floridi, R. Full, N. Jacobstein, V. Kumar, M. McNutt, R. Merrifield *et al.*, “The grand challenges of science robotics,” *Science robotics*, vol. 3, no. 14, p. eaar7650, 2018.
- [10] M. Mangan and B. Webb, “Spontaneous formation of multiple routes in individual desert ants (cataglyphis velox),” *Behavioral Ecology*, vol. 23, no. 5, pp. 944–954, 2012.
- [11] X. Sun, S. Yue, and M. Mangan, “A decentralised neural model explaining optimal integration of navigational strategies in insects,” *eLife*, vol. 9, p. e54026, jun 2020. [Online]. Available: <https://doi.org/10.7554/eLife.54026>
- [12] —, “How the insect central complex could coordinate multimodal navigation,” *Elife*, vol. 10, p. e73077, 2021.
- [13] M. Müller and R. Wehner, “Path integration in desert ants, cataglyphis fortis,” *Proceedings of the National Academy of Sciences*, vol. 85, no. 14, pp. 5287–5290, 1988.
- [14] R. Möller, “Insects could exploit uv–green contrast for landmark navigation,” *Journal of theoretical biology*, vol. 214, no. 4, pp. 619–631, 2002.
- [15] V. Aksoy and Y. Camlitepe, “Spectral sensitivities of ants—a review,” *Animal Biology*, vol. 68, no. 1, pp. 55–73, 2018.
- [16] A. Wystrach, A. Dewar, A. Philippides, and P. Graham, “How do field of view and resolution affect the information content of panoramic scenes for visual navigation? a computational investigation,” *Journal of Comparative Physiology A*, vol. 202, no. 2, pp. 87–95, 2016.
- [17] F. Steinbeck, A. Adden, and P. Graham, “Connecting brain to behaviour: a role for general purpose steering circuits in insect orientation?” *Journal of Experimental Biology*, vol. 223, no. 5, p. jeb212332, 2020.
- [18] F. Zettler and M. Järvillehto, “Lateral inhibition in an insect eye,” *Zeitschrift für vergleichende Physiologie*, vol. 76, no. 3, pp. 233–244, 1972.
- [19] B. Webb and A. Wystrach, “Neural mechanisms of insect navigation,” *Current Opinion in Insect Science*, vol. 15, pp. 27–39, 2016.
- [20] M. Heisenberg, “Mushroom body memoir: from maps to models,” *Nature Reviews Neuroscience*, vol. 4, no. 4, pp. 266–275, 2003.
- [21] A. Wystrach, M. Mangan, A. Philippides, and P. Graham, “Snapshots in ants? new interpretations of paradigmatic experiments,” *Journal of Experimental Biology*, vol. 216, no. 10, pp. 1766–1770, 2013.
- [22] L. Chittka and J. Niven, “Are bigger brains better?” *Current biology*, vol. 19, no. 21, pp. R995–R1008, 2009.
- [23] J. Zeil, M. I. Hofmann, and J. S. Chahl, “Catchment areas of panoramic snapshots in outdoor scenes,” *JOSA A*, vol. 20, no. 3, pp. 450–469, 2003.
- [24] R. Linsker, “Self-organization in a perceptual network,” *Computer*, vol. 21, no. 3, pp. 105–117, 1988.
- [25] B. Baddeley, P. Graham, P. Husbands, and A. Philippides, “A model of ant route navigation driven by scene familiarity,” *PLoS computational biology*, vol. 8, no. 1, p. e1002336, 2012.
- [26] P. Ardin, F. Peng, M. Mangan, K. Lagogiannis, and B. Webb, “Using an insect mushroom body circuit to encode route memory in complex natural environments,” *PLoS computational biology*, vol. 12, no. 2, p. e1004683, 2016.
- [27] S. Athanasoulas and A. Philippides, “Autonomous visual navigation a biologically inspired approach,” *arXiv preprint arXiv:2209.09663*, 2022.
- [28] G. J. van Dalen, K. N. McGuire, and G. C. de Croon, “Visual homing for micro aerial vehicles using scene familiarity,” *Unmanned Systems*, vol. 6, no. 02, pp. 119–130, 2018.
- [29] D. D. Gaffin and B. P. Brayfield, “Autonomous visual navigation of an indoor environment using a parsimonious, insect inspired familiarity algorithm,” *Plos one*, vol. 11, no. 4, p. e0153706, 2016.
- [30] J. C. Knight, D. Sakhapov, N. Domcsek, A. D. Dewar, P. Graham, T. Nowotny, and A. Philippides, “Insect-inspired visual navigation on-board an autonomous robot: Real-world routes encoded in a single layer network,” in *ALIFE 2019: The 2019 Conference on Artificial Life.* MIT Press, 2019, pp. 60–67.
- [31] L. Zhu, M. Mangan, and B. Webb, “Spatio-temporal memory for navigation in a mushroom body model,” in *Conference on Biomimetic and Biohybrid Systems.* Springer, 2020, pp. 415–426.
- [32] J. K. Verheyen, J. Dupeyroux, and G. C. d. Croon, “A novel multi-vision sensor dataset for insect-inspired outdoor autonomous navigation,” in *Biomimetic and Biohybrid Systems: 11th International Conference, Living Machines 2022, Virtual Event, July 19–22, 2022, Proceedings.* Springer, 2022, pp. 279–291.
- [33] A. Kodzhabashev and M. Mangan, “Route following without scanning,” in *Conference on Biomimetic and Biohybrid Systems.* Springer, 2015, pp. 199–210.
- [34] F. Le Möel and A. Wystrach, “Opponent processes in visual memories: A model of attraction and repulsion in navigating insects’ mushroom bodies,” *PLoS computational biology*, vol. 16, no. 2, p. e1007631, 2020.
- [35] A. Wystrach, G. Beugnon, and K. Cheng, “Ants might use different view-matching strategies on and off the route,” *Journal of Experimental Biology*, vol. 215, no. 1, pp. 44–55, 2012.